Plant Physiol. (1989) 89, 27–36
0032-0889/89/89/0027/010/$01.00/0

Received for publication February 18, 1988
and in revised form August 1, 1988

Regulation of Vacuolar pH of Plant Cells

II. A ^{31}P NMR Study of the Modifications of Vacuolar pH in Isolated Vacuoles Induced by Proton Pumping and Cation/H^+ Exchanges

Jean Guern*, Yves Mathieu, Armen Kurkdjian, Pierre Manigault, Jeanne Manigault, Brigitte Gillet, Jean-Claude Beloeil, and Jean-Yves Lallemand

Laboratoire de Physiologie Cellulaire Végétale, CNRS, 91198, Gif-sur-Yvette cedex, France (J.G., Y.M., A.K., P.M., J.M.), *and Institut de Chimie des Substances Naturelles, Laboratoire de RMN, CNRS, 91198 Gif-sur-Yvette cedex, France* (B.G., J.-C.B., J.-Y.L.)

ABSTRACT

The vacuolar pH and the *trans*-tonoplast ΔpH modifications induced by the activity of the two proton pumps H^+-ATPase and H^+-PPase and by the proton exchanges catalyzed by the Na^+/H^+ and Ca^{2+}/H^+ antiports at the tonoplast of isolated intact vacuoles prepared from *Catharanthus roseus* cells enriched in inorganic phosphate (Y Mathieu et al 1988 Plant Physiol [in press]) were measured using the ^{31}P NMR technique. The H^+-ATPase induced an intravacuolar acidification as large as 0.8 pH unit, building a *trans*-tonoplast ΔpH up to 2.2 pH units. The hydrolysis of the phosphorylated substrate and the vacuolar acidification were monitored simultaneously to estimate kinetically the apparent stoichiometry between the vectorial proton pumping and the hydrolytic activity of the H^+-ATPase. A ratio of H^+ translocated/ATP hydrolyzed of 1.97 ± 0.06 (mean ± standard error) was calculated. Pyrophosphate-treated vacuoles were also acidified to a significant extent. The H^+-PPase at 2 millimolar PPi displayed hydrolytic and vectorial activities comparable to those of the H^+-ATPase, building a steady state ΔpH of 2.1 pH units. Vacuoles incubated in the presence of 10 millimolar Na^+ were alkalinized by 0.4 to 0.8 pH unit. It has been shown by using ^{23}Na NMR that sodium uptake was coupled to the H^+ efflux and occurred against rather large concentration gradients. For the first time, the activity of the Ca^{2+}/H^+ antiport has been measured on isolated intact vacuoles. Ca^{2+} uptake was strongly inhibited by NH_4Cl or gramicidin. Vacuoles incubated with 1 millimolar Ca^{2+} were alkalinized by about 0.6 pH unit and this H^+ efflux was associated to a Ca^{2+} uptake as demonstrated by measuring the external Ca^{2+} concentration with a calcium specific electrode. Steady state accumulation ratios of Ca^{2+} as high as 100 were reached for steady state external concentrations about 200 micromolar. The rate of Ca^{2+} uptake appeared markedly amplified in intact vacuoles when compared to tonoplast vesicles but the antiport displayed a much lower affinity for calcium. The different behavior of intact vacuoles compared to vesicles appears mainly to be due to differences in the surface to volume ratio and in the rates of dissipation of the pH gradient. Despite its low affinity, the Ca^{2+}/H^+ antiport has a high potential capacity to regulate cytoplasmic concentration of calcium.

Studies during the past few years have shown that the tonoplast is endowed with a complex set of primary and secondary H^+ transport systems associated with cation accumulation and anion retrieval (6). However, aside the relatively well studied tonoplast proton pumping ATPase (26, 28 and references therein), our knowledge of the other ionic exchanges involving fluxes of protons or proton-equivalents is more limited. A second proton pump, the H^+-PPase, present on tonoplast-enriched microsomal vesicles, has been described several times as distinct from the H^+-ATPase (12, 25, 31). Its hydrolytic activity has also been measured on isolated intact vacuoles of beet roots (32) and tulipa petals (31) but, in these few cases, the possible effect of PPi hydrolysis on the vacuolar pH has not been determined.

The study of H^+-coupled secondary transport of cations through the functioning of Na^+/H^+ or Ca^{2+}/H^+ antiports has been restricted to tonoplast vesicles isolated from beet (8, 9) carrot (11), or oat (27) roots. Their activity in isolated, intact vacuoles has only been measured in very few cases (7) and their potential importance in the regulation of vacuolar pH and of cytosolic ionic content remains largely unknown.

Most of our knowledge of the functional units present at the tonoplast is derived from elegant experiments performed with tonoplast-enriched microsomal vesicles or tonoplast vesicles prepared from vacuoles. We provide here data concerning intact vacuoles, isolated from *Catharanthus roseus* cells, which, due to their much lower surface to volume ratio compared to vesicles and to their natural ionic composition and buffering components, present conditions that are different from those in isolated vesicles and more closely related to those of vacuoles *in situ*.

Finally, the techniques used to study the exchanges of protons at the tonoplast have been in most cases based on the intravesicular ΔpH-driven accumulation of fluorescent or radioactive weak bases. These efficient and sensitive techniques are difficult to calibrate in order to measure the intravesicular H^+-concentration, the transmembrane ΔpH value and their variations. We show here that the ^{31}P NMR technique largely overcomes these limitations and can be used to measure the modifications of vacuolar pH and *trans*-tonoplast ΔpH associated with the exchange of protons or proton-equivalents at the tonoplast in intact vacuoles.

MATERIALS AND METHODS

Unless otherwise indicated, the isolation of Pi-enriched vacuoles from *Catharanthus roseus* cell suspensions was done

as described in the first paper of this series (22). In some experiments, as indicated in the text and figure legends, the isolation procedure was modified as follows. The stabilization medium consisted of 9 mL of 8% Ficoll, Hepes-KOH (10 mM, pH 7.8) adjusted to 640 mosm with sorbitol, giving a final osmolarity of 550 mosm in the lower phase of the gradient. This lower phase was overlayed with 1 mL 4% Ficoll in the same buffer adjusted to 550 mosm with sorbitol, itself overlayed with 1 mL of BTP-Mes buffer (25 mM, pH 7.8) containing KCl 50 mM, DTT 1 mM, BSA 1 mg·mL^{-1}, again adjusted to 550 mosm with sorbitol. This three-step gradient was centrifuged for 10 min at 650*g*. Vacuoles were recovered at the 0 to 4% Ficoll interface.

The conditions for ^{31}P NMR measurements have been described in a preceding paper (22). ^{23}Na NMR spectra were obtained at 105.84 MHz with a 20 mm diameter broadband probe. The intravacuolar and extravacuolar ^{23}Na signals were separated by using the shift reagent K_7 Dy(PPPi)$_2$[1] according to Martin *et al.* (21). Na^+ was estimated by comparison of the area of the peaks to those corresponding to calibrated NaCl solutions.

Uptake of Ca^{2+} by isolated vacuoles was determined with 1 mL of vacuole suspension (about 2×10^6 vacuoles) by using a Ca^{2+}-specific electrode (Radiometer F 2112 Ca). Signal output was measured with a digital ion analyzer (Ion 85 ion analyzer, Radiometer) coupled to a REC 80 servograph (Radiometer). The amount of Ca^{2+} taken up was determined by back titration with a Ca^{2+} standard solution. The sensitivity of the electrode was close to the Nernstian slope factor (29 mV/decade) for Ca^{2+} concentrations down to 0.1 mM but markedly decreased for lower Ca^{2+} concentrations.

RESULTS AND DISCUSSION

Study of the Vectorial H^+-ATPase at the Tonoplast of Vacuoles Isolated from *Catharanthus roseus* Cells

Figure 1 illustrates the evolution with time of ^{31}P NMR spectra of a vacuolar suspension incubated with Mg-ATP. The extravacuolar and intravacuolar inorganic phosphate peaks were clearly distinct from the peaks corresponding to the three phosphate groups of ATP. As ATP was hydrolyzed, the two ADP peaks appeared along with a weak AMP signal. The main interest of using ^{31}P NMR was that it allowed simultaneously (a) the measurement of ATP hydrolysis, (b) the measurement of vacuolar pH modifications linked to ATP hydrolysis, and (c) the estimation of the apparent stoichiometry between vectorial H^+-pumping and the hydrolytic activities of the H^+-ATPase.

The rate of ATP hydrolysis was measured from the evolution with time of the area of the β-ATP peak. The ADP, AMP, and Pi formations were also determined from the same spectra. Figure 2 illustrates a typical experiment showing that during the first 30 min of incubation a good correlation was observed between ATP hydrolysis and appearance of ADP and Pi, with a limited accumulation of AMP issued from the further hydrolysis of ADP. Later on, the kinetics were more

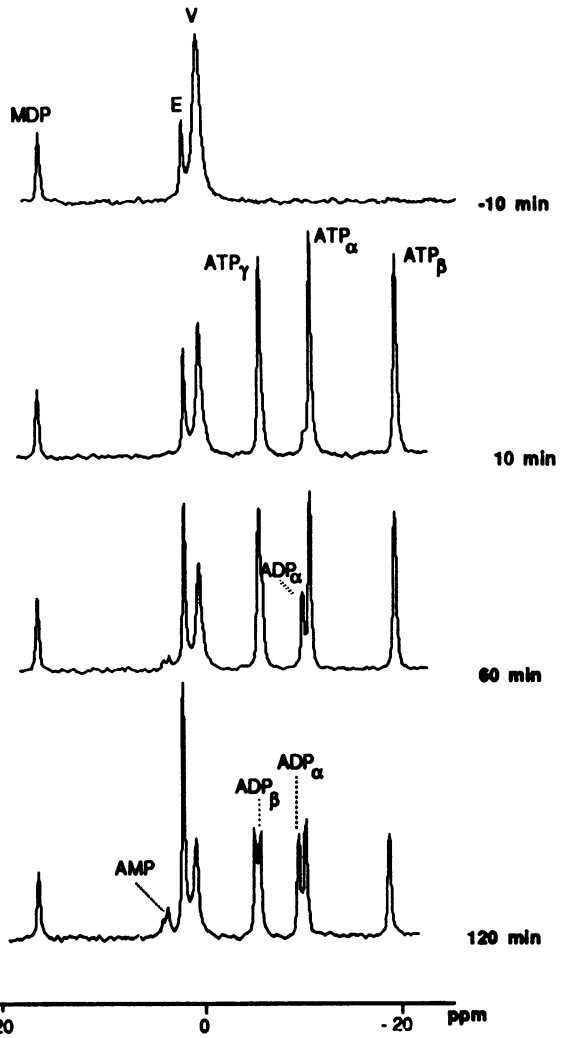

Figure 1. Successive ^{31}P NMR spectra of a vacuolar preparation incubated in the presence of Mg-ATP. The vacuoles were isolated and collected in a BTP Mes buffer (25 mM, pH 7.5) as described (22). The NMR tube contained 3×10^7 vacuoles in a 12 mL suspension (pHe = 7.03). At time zero, 2 mM Mg-ATP, 0.5 mM K^+ molybdate, and 5 mM $MgCl_2$ were injected in the tube. Each spectrum corresponds to an acquisition time of 10 min taken 10 min before the addition of ATP and after 10, 60, and 120 min in the presence of ATP, ATP α,β,γ; ADP α,β correspond, respectively, to the alpha, beta, gamma phosphate groups of ATP and to the alpha and beta phosphate groups of ADP. V and E correspond, respectively, to the vacuolar and external inorganic phosphate. MDP is the reference peak of a 100 mM methylene diphosphonate solution contained in a capillary tube.

complex with a marked decrease in the rate of ADP accumulation and an increase in AMP formation. The mean rates of ATP hydrolysis, ADP, and Pi formation calculated from the first 30 min of incubation in a series of experiments are given in Table I. They demonstrate that unspecific phosphatases were efficiently inhibited by the molybdate ions added to the suspension and that the ATP hydrolysis measured during this period could be essentially attributed to the ATPase activity.

The rate of ATP hydrolysis was 0.19 ± 0.02 μmol Pi·h^{-1}·10^6 vacuoles (mean ± SE), *i.e.* about 27 to 50 μmol Pi·h^{-1}·

[1] Abbreviations: Dy(PPPi)$_2^{7-}$, bis (tripolyphosphate) dysprosium III; CCCP, carbonylcyanide-*m*-chlorophenylhydrazone; FCCP, carbonylcyanide *p*-trifluoromethoxyphenylhydrazone; PPase, pyrophosphatase; pHe, external pH; pHv, vacuolar pH.

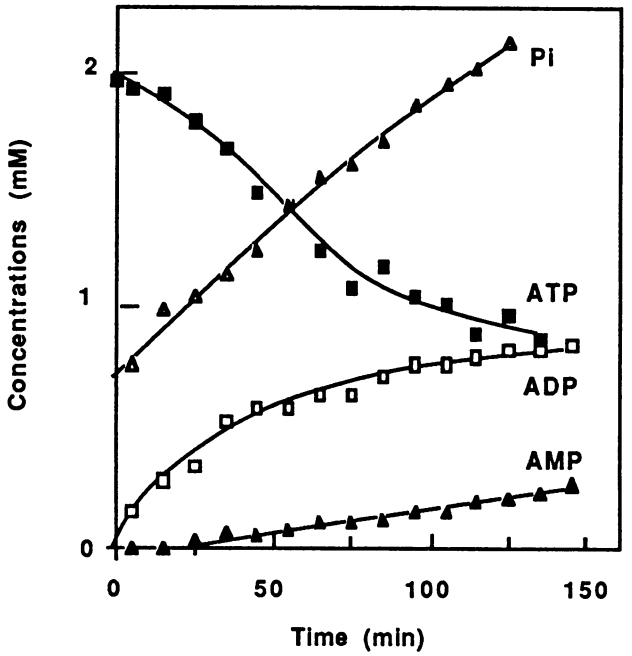

Figure 2. Kinetics of the hydrolysis of ATP and appearance of ADP, AMP, and Pi in a vacuolar preparation as determined by ^{31}P NMR. The NMR tube contained 3×10^7 vacuoles in 12 mL suspension. Conditions are the same as in Figure 1. The kinetics were followed by taking successive 10 min spectra. Concentrations of ATP, ADP, AMP, and Pi were calculated by measuring the relative areas under the peaks corresponding to the βATP, αADP, AMP, and Pi phosphate groups, respectively.

Table I. *Comparison of the Rates of ATP Hydrolysis, ADP Accumulation and Inorganic Phosphate Increase in Vacuolar Preparations of C. roseus Cells*

Mg-ATP was injected in the vacuolar suspension to a final concentration of 2 mM and its metabolism was monitored by measuring the area of the peaks corresponding to the β-ATP, α-ADP and inorganic phosphate groups. Rates were calculated from the first 30 min of incubation and expressed as $\mu mol \cdot h^{-1} \cdot 10^6$ vacuoles (mean ± SE).

ATP Hydrolysis	ADP Formation	Pi Formation
0.195 ± 0.02	0.190 ± 0.02	0.192 ± 0.03

mg^{-1} tonoplastic proteins in agreement with the values reported in the literature for tonoplast vesicles (3, 10, 16, 25) and for isolated vacuoles (1, 16, 19, 24, 32).

The ATP-induced acidification of *C. roseus* vacuoles isolated in BTP-Mes buffer without KCl was small (0.2–0.3 pH unit) and rather variable. In contrast, when vacuoles were isolated in the presence of KCl 50 mM, according to the modified procedure (see "Materials and Methods"), the amplitude of the acidification was much higher (0.80 ± 0.03 pH unit; mean ± SE). The intensity of the vacuolar acidification observed in these conditions (Fig. 3) appeared higher than most of the acidifications reported for ATP-treated intact vacuoles (13, 23, 29). Vacuoles isolated from *C. roseus* cells were able to build a large *trans*-tonoplast ΔpH: starting from a mean ΔpH of 1.56 ± 0.07 (22), ATP-treated vacuoles increased their proton gradient up to 2.25 ± 0.13 pH units, a

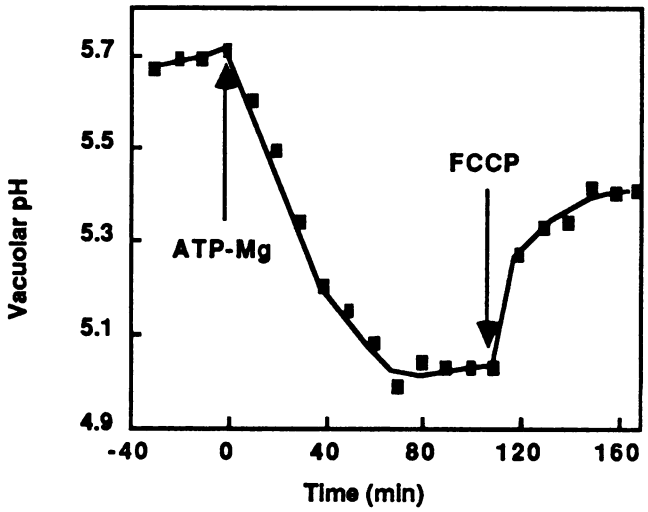

Figure 3. Kinetics of vacuolar acidification in the presence of ATP. Vacuoles were collected by flotation in a BTP Mes buffer (25 mM, pH 7.8) containing 50 mM KCl, 1 mM DTT, 1 $mg \cdot mL^{-1}$ BSA as described in "Material and Methods." The NMR tube contained 1.9×10^7 vacuoles in a 12 mL suspension (pHe = 7.25). Stability of the vacuolar preparation was first checked by taking four successive spectra of 10 min each. At time indicated by the first arrow, the vacuolar acidification was initiated by simultaneously adding 2 mM MgATP and 0.5 mM K_2MoO_4 and the vacuolar acidification was followed for about 2 h. At time indicated by the second arrow, FCCP (10 μM) was injected into the vacuole suspension and the subsequent vacuolar alkalinization was followed for 1 h.

value as large as the one described for *Chenopodium rubrum* vacuoles (5). Addition of FCCP (10 μM) to the vacuolar preparations partially abolished the ATP-induced acidification of the vacuoles. DCCD (100 μM) totally reversed the ATP-induced acidification (results not shown). Nitrate (50 mM) inhibited the hydrolysis of ATP by 50% and induced an alkalinization (+0.35 pH unit after 2.5 h) of vacuoles prepared according to the standard procedure.

A characteristic feature of the ATP-induced acidification of intact vacuoles was its apparently low rate compared to the one reported for tonoplast vesicles. The half-maximum change in pHv was observed after about 30 min (Fig. 3) whereas half-maximum variation of the quenching of ΔpH probes in vesicles was obtained after about 2 to 4 min or less (25). This likely corresponds to the much greater surface to volume ratio for vesicles than for the vacuoles, *i.e.* about 25- to 80-fold, for a mean diameter of 0.3 to 1 μm (2) and 25 μm, respectively.

Another original aspect of the NMR approach was that it allowed the simultaneous measurement of the ATP hydrolysis and the vacuolar acidification and consequently the estimation of the ratio of H^+ transported to ATP hydrolyzed. Table II shows that the ratio H^+/ATP calculated for three different experiments from the rates of ATP hydrolysis and vacuolar acidification measured during the first 30 min of incubation was close to 2 (mean ± SE = 1.97 ± 0.06). This ratio is, of course, strongly dependent on the value of the buffering capacity chosen for the calculation. The buffering capacity β of the vacuolar sap around pH 5.5 calculated from the malate, citrate, and phosphate contents was in good agreement with the one estimated from weak base-induced alkalinizations

Table II. *Tentative Estimation of the Apparent Stoichiometry between ATP-Induced Proton Influx in Isolated Vacuoles of C. roseus Cells and ATP Hydrolysis*

The initial rates of ATP hydrolysis were measured from the evolution with time of the β-ATP peak of the ^{31}P NMR spectra during the first 20 to 30 min of incubation and expressed as ΔATP ($\mu mol \cdot h^{-1}$) hydrolyzed per 10^6 vacuoles. The initial rates of acidification were measured on the same spectra from the first 30 min of acidification and expressed as ΔpH (pH unit$\cdot h^{-1}$). From the buffering capacity of the vacuolar sap (β = 36 $\mu Eq \cdot H^+ \cdot mL^{-1} \cdot$ pH unit^{-1}) and the internal volume corresponding to 10^6 vacuoles (v = 11.6 ± 1 μL), the rates of ATP-induced proton injection into the vacuole were calculated as $\Delta H^+ = \beta \times \Delta pH \times v$.

Experiment	ΔATP	ΔpH	ΔH^+	$\Delta H^+/\Delta ATP$
	$\mu mol \cdot h^{-1}$	pH unit$\cdot h^{-1}$	$\mu Eq \cdot h^{-1}$	
A	0.19	0.85	0.355	1.87
B	0.16	0.80	0.334	2.09
C	0.16	0.75	0.313	1.96

(22). Extrapolation of these calculations of β values in the range pH 5.0 to 5.5 showed that a mean value of 36 $\mu Eq \cdot ml^{-1} \cdot$ pH unit^{-1} (22) could be considered as reasonably valid for the ATP-induced acidification.

Contrary to Bennett and Spanswick (4) who calculated the H^+/ATP ratio for the NO_3^--sensitive fractions of the hydrolytic and vectorial activities of the H^+-ATPase of tonoplast-enriched beet root vesicles, we estimated the apparent stoichiometry in the absence of nitrate. The main reason was that a differential inhibition by NO_3^- of the H^+-transport and ATP hydrolysis (H^+ transport being more sensitive) has been observed several times (18, 30). Furthermore, the contaminating phosphatase activity of *C. roseus* vacuole preparations which could lower the H^+/ATP stoichiometry (4), was low as revealed by the slow hydrolysis of ADP formed during the first 30 min of incubation (Table I). This is the first apparent stoichiometry estimated using intact vacuoles and the ratio H^+/ATP close to 2 is in good agreement with the ratio determined by Bennett and Spanswick (4) for the H^+-ATPase of beet root tonoplast.

Study of the Vectorial H^+-PPase at the Tonoplast of Vacuoles Isolated from *C. roseus* Cells

When *C. roseus* vacuoles were incubated with 2 mM pyrophosphate, the ^{31}P NMR spectra displayed a characteristic pattern with the two Pi peaks corresponding to the external and intravacuolar inorganic phosphate pools and a distinct pyrophosphate peak at −5.86 ppm (pHe = 7.52). Thus, it was possible to monitor from the same spectra the PPi-induced modifications of vacuolar pH (Fig. 4A) and the hydrolysis of the substrate pyrophosphate (Fig. 4B). PPi-induced vacuolar acidification was reversed by the addition of CCCP (10 μM) whereas PPi hydrolysis was stimulated by 50%. The optimal conditions for the activity of the H^+-PPase in terms of PPi concentration and PPi/Mg^{2+} ratio were not determined. Thus, we did not attempt to estimate the stoichiometry between the vectorial H^+-pumping and hydrolytic activities of the PPase as it appears from the literature that the activity of the H^+-PPase and the ratio H^+ translocated/PPi hydrolyzed can be strongly dependent on the PPi and Mg^{2+} concentrations (17).

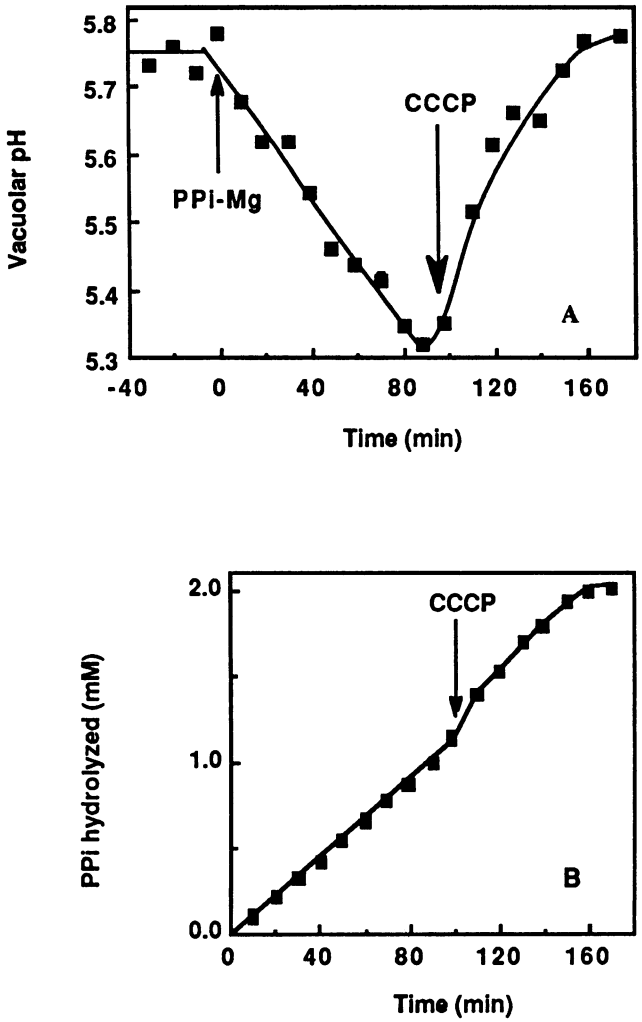

Figure 4. Kinetics of pyrophosphate-induced vacuolar acidification and pyrophosphate hydrolysis. Vacuoles collected as described in Figure 3 were first incubated for 40 min (A) to check the stability of their vacuolar pH. The NMR tube contained 2.6 × 10^7 vacuoles in a 12 mL suspension (pHe = 7.48). Vacuolar acidification was initiated by simultaneously adding 2 mM PPi, 2 mM $MgSO_4$, and 0.5 mM K_2MoO_4 (first arrow). At time indicated by the second arrow, CCCP (10 μM) was injected into the vacuole suspension and the subsequent vacuolar alkalinization was followed for 70 min. In the same conditions and on the same spectra, PPi hydrolysis was followed by determining the increase of the area of the peak corresponding to the external Pi resonance (B).

The hydrolytic activity of the H^+-PPase measured for a PPi concentration of 2 mM and a PPi/Mg^{2+} ratio of 1 (0.18 ± 0.03 $\mu mol\ PPi \cdot h^{-1} \cdot 10^6$ vacuoles, *i.e.* about 25 to 50 $\mu mol\ PPi \cdot h^{-1} \cdot mg^{-1}$ protein) was higher than the values reported for oat root (33) and beet root vesicles (3) and comparable to the rate of ATP hydrolysis catalyzed by the ATPase. The vectorial activity of the H^+-PPase resulted in a marked acidification of the vacuolar sap (Fig. 4A) which, given the rather high buffering capacity of the sap, corresponded to a high proton flux. Because of the higher external pH used for testing the H^+-PPase activity, the maximal *trans*-tonoplast pH gradient built under the influence of the H^+-PPase (ΔpH = 2.0

and 2.14 in two separate experiments) was of the same order of magnitude as the one measured for the H^+-ATPase.

Thus, in *C. roseus* vacuoles the two proton pumps, H^+-ATPase and H^+-PPase, have similar capacities for building steady state ΔpH values (respectively 2.2 and 2.1 pH units) in good agreement with the values of 1.4 and 2.0 reported for beet root vesicles (26).

The fact that the H^+-ATPase and H^+-PPase reside at the same membrane has been discussed several times (17, 26) starting from the idea that the two enzymes could be associated with different subpopulations of the tonoplast-enriched microsomal vesicles (12). The results obtained here on intact vacuoles of *C. roseus* are devoid of such ambiguity as the ^{31}P NMR signals are almost entirely due to the large intact vacuoles of the preparation and do not arise from the vesicles derived from burst vacuoles.

Evidence for the Operation of a Na^+/H^+ Antiport at the Tonoplast of Vacuoles Isolated from Pi-Loaded *C. roseus* Cells

Figure 5 shows that the addition of Na_2SO_4 (5 mM) to a vacuolar suspension induced a marked increase of the vacuolar pH. NaCl (10 mM) induced an increase of the vacuolar

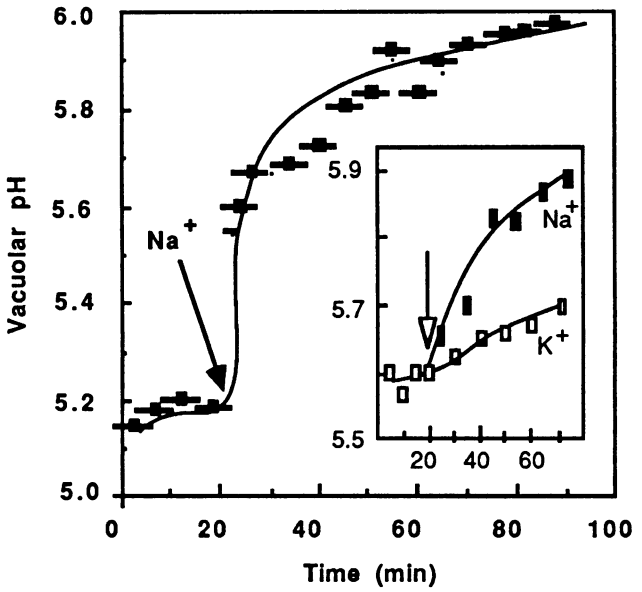

Figure 5. Effect of Na^+ uptake on the internal pH of isolated vacuoles. The vacuoles were obtained as described (22). The NMR tube contained 2×10^7 vacuoles in a 12 mL suspension (pHe = 7.08). Each bar represents the pH value obtained from elementary spectra accumulated for 10 min. At time indicated by arrow, Na_2SO_4 (5 mM) was injected in the vacuolar preparation and the evolution of pHv was monitored. (Inset): Comparison of the effect of Na_2SO_4 (5 mM) and K_2SO_4 (5 mM) on the vacuolar pH of isolated vacuoles. Kinetics of the pH changes were followed by alternately measuring the pHv on two aliquots of the same vacuolar preparation treated either with Na_2SO_4 or K_2SO_4. Five mL of the vacuolar preparation (about 10^7 vacuoles) were put in a 15 mm diameter NMR tube. This tube was inserted in the 20 mm diameter tube. The inner tube was surrounded by 4 mL of the buffer medium used for the recovery of the vacuoles and containing the same concentration of D_2O as the inner tube (17%).

pH similar to the one obtained with Na_2SO_4 (results not shown). The vacuolar alkalinization induced by 50 mM Na^+ was similar to the one obtained with 10 mM Na^+ (data not shown) suggesting that the observed Na^+-induced pH increase was a saturable process. Figure 5 (inset) shows that K^+ (10 mM) was less effective than Na^+ (10 mM) in inducing vacuolar alkalinization as observed for tonoplast vesicles of beet roots (8).

Such results are in good agreement with those obtained by Blumwald and Poole (8) demonstrating the alkalinization of tonoplast vesicles isolated from sugar beet through the functioning of a Na^+/H^+ antiport. The kinetics of vacuolar pH variations are much slower than those reported for isolated tonoplast vesicles where 50% of maximum quenching of the ΔpH probe (acridine orange) was obtained after about 0.5 to 1 min compared to the 10 to 20 min necessary to obtain the half-maximum change of pH_v in intact vacuoles (Fig. 5). As discussed above, this difference is likely linked to the lower surface to volume ratio for intact vacuoles compared to vesicles. The steady state vacuolar alkalinization induced by 10 mM Na^+, which was rather variable (0.35–0.7 pH unit), corresponded to a significant proton efflux when compared to the capacity of pumping of the H^+-ATPase. In agreement with the report that external Na^+ inhibits the ATP-induced acidification of intact red beet vacuoles (23) our results suggest that because of the strong potential activity of the Na^+/H^+ antiport, the ATP-induced acidification could be significantly antagonized by the presence of Na^+ ions in the suspension medium.

To test the hypothesis that the loss of H^+ from the vacuolar sap was linked to an influx of Na^+, the intravacuolar Na^+ content was monitored by ^{23}Na NMR, using K_7 Dy(PPPi)$_2$ as a shift reagent to separate the intravacuolar and external Na^+ signals (21). Figure 6 illustrates a typical ^{23}Na NMR spectrum of control vacuoles with only a clear intravacuolar sodium peak (a) and a spectrum of vacuoles incubated for 40 min with 10 mM Na^+ displaying the two peaks corresponding to the internal and external Na^+ pools (b). Under these conditions, the intravacuolar Na^+ concentration at equilibrium was increased by about 8 to 10 mM for a final concentration of 45 to 50 mM.

Assuming that one H^+ was exchanged against one Na^+ taken up, the vacuolar alkalinization of 0.35 pH unit observed at equilibrium (Fig. 5) should correspond to an increase of the vacuolar Na^+ concentration of 13 mM, in reasonably good agreement with the experimental results. Thus, the accumulation of sodium, linked to the H^+-efflux and driven by an initial *trans*-tonoplast pH gradient of 1.5 pH unit, was achieved against a *trans*-tonoplast Na^+ concentration gradient of four- to fivefold. This is in good agreement with the accumulation ratio predicted by Blumwald and Poole (8) from the pH-dependent affinity of the antiport for Na^+ at the two faces of the tonoplast membrane.

Evidence for the Operation of a Ca^{2+}/H^+ Antiport at the Tonoplast of Vacuoles Isolated from Pi-Loaded *C. roseus* Cells

The addition of 1 mM Ca^{2+} to a suspension of vacuoles isolated from *C. roseus* cells induced a strong dissipation (about 50%) of the *trans*-tonoplast ΔpH (Fig. 7). No signifi-

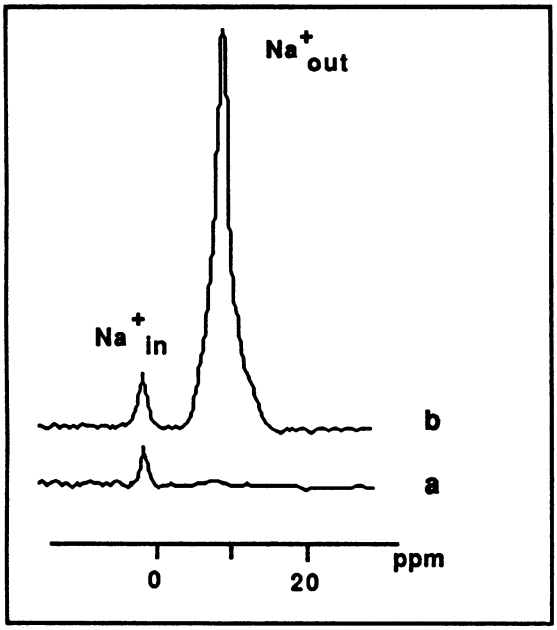

Figure 6. Uptake of Na^+ by isolated vacuoles. The vacuoles were obtained as described (22). The uptake was determined by $^{23}Na^+$ NMR using the shift reagent $K_7Dy(PPPi)_2$ (2.5 mM) to distinguish between external and internal Na^+. The NMR tube contained 2.4×10^7 vacuoles in a 12 mL suspension. Spectra correspond to 500 scans of 0.6 s each. a, Control vacuolar preparation. Vacuolar Na^+ was determined to be about 38 mM; b, vacuolar preparation incubated for 40 min in the presence of 10 mM NaCl. The vacuolar Na^+ was then determined to be about 46 mM.

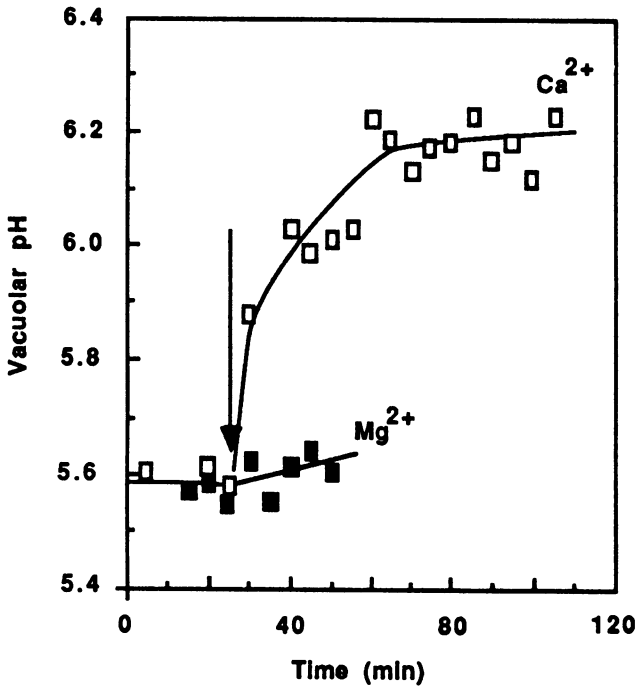

Figure 7. Comparison of the effect of $CaCl_2$ and $MgCl_2$ on the internal pH of isolated vacuoles. The vacuoles were obtained as described (22). Kinetics of pH changes were followed by accumulating elementary spectra during 10 min. At time indicated by arrow $MgCl_2$ or $CaCl_2$ (1 mM final concentration) was injected in the NMR tube. Numbers of vacuoles were 2.3×10^7 (Ca^{2+}) and 2.1×10^7 (Mg^{2+}) in 12 mL suspension. External pH values were 6.95 and 7.20 for Ca^{2+} and Mg^{2+} treatments, respectively.

cant alkalinization of the vacuoles was obtained after addition of 1 mM Mg^{2+}. Furthermore, the calcium-induced alkalinization was not inhibited by the presence of 2 mM Mg^{2+} (data not shown).

The same alkalinization was observed when the internal pH of Ca^{2+}-treated vacuoles was measured on individual vacuoles by 9-aminoacridine microfluorimetry. The heterogeneity of the vacuolar populations in terms of internal pH revealed by this technique (about 1 pH unit difference between the most and the less acidic vacuoles of the same population) was not modified by the calcium treatment. All vacuoles were apparently alkalinized to the same extent, irrespective of their initial internal pH (Fig. 8). The same behavior has already been described for the fusicoccin-induced vacuolar alkalinization of *Acer pseudoplatanus* cells (14) and a simple model accounting for the distribution of vacuolar pH values in populations of cells, protoplasts or isolated vacuoles has been proposed (15).

The Ca^{2+}-induced vacuolar alkalinization is likely resulting from a Ca^{2+}-driven proton efflux through a Ca^{2+}/H^+ antiport analogous to the one described on tonoplast vesicles isolated from carrot cells (11), storage tissue of beet (9), and oat roots (27). *C. roseus* vacuoles were able to take up Ca^{2+} with a capacity high enough to induce a marked decrease of the extravacuolar Ca^{2+} concentration (Fig. 9) and a time course reasonably consistent with that of the pH changes. The amount of calcium accumulated under these conditions corresponded to an increase of the intravacuolar Ca^{2+} concentration (ΔCi) of about 20 mM for 200 μM external calcium at equilibrium. Thus, Ca^{2+} ions were taken up against a strong concentration gradient ($\Delta Ci/Ce = 101 \pm 5$ at equilibrium; three experiments), likely driven by the *trans*-tonoplast ΔpH. The fact that the uptake of Ca^{2+} was dependent on the *trans*-tonoplast ΔpH was supported by the strong reduction (at least 10-fold) of the rate of calcium uptake induced by addition of NH_4Cl (10 mM) or gramicidin (10 $\mu g \cdot ml^{-1}$) to the vacuolar suspension (results not shown).

The apparent stoichiometry between the uptake of Ca^{2+} and the corresponding efflux of protons was first tentatively estimated from the rates of vacuolar alkalinization and Ca^{2+} uptake measured during the first 10 min after adding calcium (0.5–0.8 mM) to the vacuole suspension. Due to the rapidity of the vacuolar alkalinization compared to the duration of each measurement, only maximum and minimum values of the rate of H^+ efflux could be estimated (2.36 ± 0.4 to 4.72 ± 0.8 pH units$\cdot h^{-1}$, *i.e.* 90 ± 15 to 180 ± 30 $\mu Eq \cdot H^+ \cdot h^{-1} \cdot mL^{-1}$). The mean rate of Ca^{2+} uptake estimated for a number of vacuoles corresponding to a cumulative internal volume of 1 mL was 95.6 ± 3.4 /mol$\cdot h^{-1} \cdot mL^{-1}$. The range of Ca^{2+}/H^+ ratios calculated from these values was 0.58 to 1.06. A different estimation of the apparent stoichiometry of the Ca^{2+}/H^+ exchange was made from ΔH^+ and ΔCa^{2+} at equilibrium for 0.8 mM external calcium. The mean ΔpH was 0.63 ± 0.10 pH units (five experiments). The corresponding loss of protons was estimated as $\Delta H^+ = 31.6 \pm 4.1$ $\mu Eq \cdot mL^{-1}$, taking into account and calculating as described (22) the increase of the buffering capacity above pH 6. The mean ΔCa^2 for a

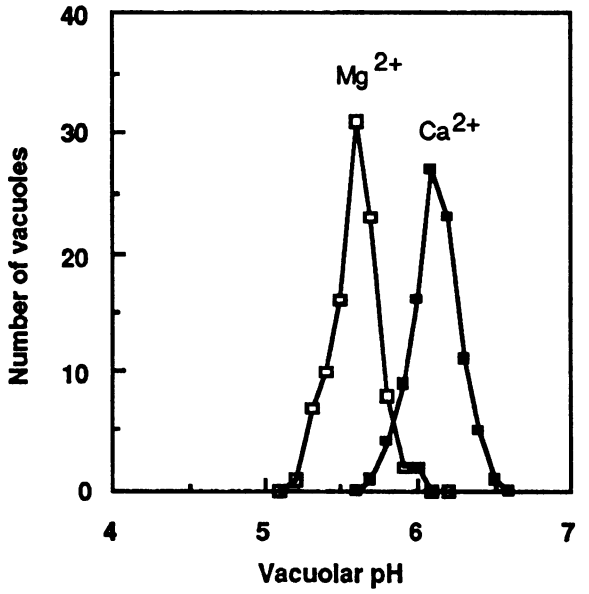

Figure 8. Influence of Ca^{2+} on the distribution of pH values in populations of vacuoles isolated from *C. roseus* cells. A vacuolar suspension (2.3×10^6 vacuoles·mL^{-1}) isolated from Pi-loaded cells was separated in two aliquots incubated for 1 h either with Mg^{2+} 1 mM or with Ca^{2+} 1 mM. The pH probe 9-aminoacridine (5 μM) was then added and the vacuoles incubated for 45 to 60 min until the diffusion equilibrium of the probe was reached. The vacuolar pH values were determined by microfluorimetric measurements of the external and intravacuolar concentrations of 9AA and by the calculation of the accumulation ratio of the probe according to Manigault *et al.* (20). The pH values corresponding to individual vacuoles were grouped by classes and the number of vacuoles corresponding to each class plotted as ordinates. The mean vacuolar pH of Ca^{2+}-treated vacuoles was 6.14, 0.52 pH unit higher than the one corresponding to the vacuoles treated with Mg^{2+}. External pH values were 7.1 and 6.9 for Ca^{2+} and Mg^{2+} treatments, respectively.

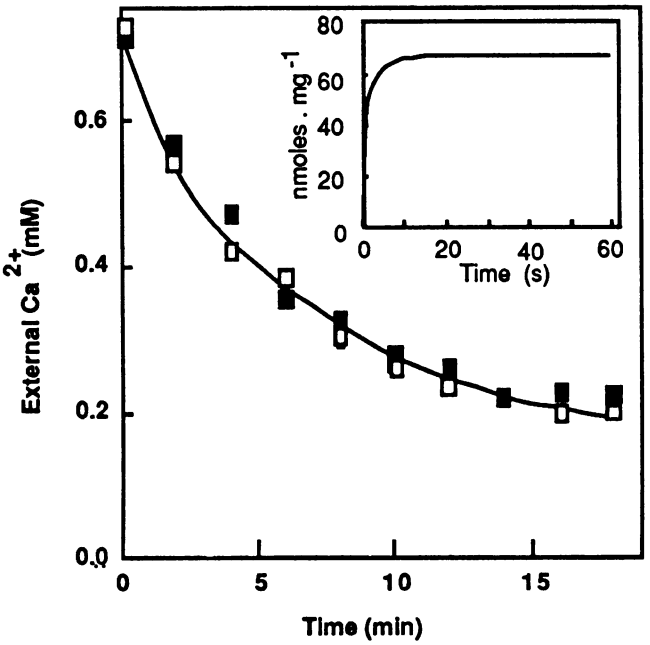

Figure 9. Time course of the disappearance of external Ca^{2+} linked to Ca^{2+} uptake by isolated vacuoles. At time 0, $CaCl_2$ was injected to a final concentration of 0.7 mM into 1 mL of a vacuolar suspension containing 2×10^6 vacuoles obtained as described (22). The output signal of the Ca^{2+} specific electrode was converted into Ca^{2+} concentration values by using a calibration curve, itself checked in each experiment by a stepwise back titration. During measurement, the vacuolar suspension was continuously agitated. The different symbols correspond to experimental results from distinct experiments. Solid line corresponds to the predicted Ca^{2+} uptake by a 1 mL suspension containing 2×10^6 vacuoles, with a mean diameter of 27 μm and an initial *trans*-tonoplast ΔpH of 1.8 pH unit (pHv = 5.5), using the model described in the legend of Figure 10 and in the text. The same model, with the same kinetic parameters was used to calculate what should be the time course of Ca^{2+} uptake (nmol Ca^{2+} absorbed per mg tonoplast proteins) by tonoplast vesicles with a mean diameter of 0.3 μm, an initial *trans*-tonoplast ΔpH of 1.9 pH unit (initial intravesicular pH:5.4) and an intravesicular buffering capacity of 4 μEq·mL^{-1} pH unit^{-1} around pH 5.5 (inset).

number of vacuoles corresponding to an internal volume of 1 mL was 17.2 ± 0.4 μmol·mL^{-1} (five experiments). The Ca^{2+}/H^+ ratio calculated from these values was 0.54. This estimation based on the equilibrium conditions is at first sight more precise than the one derived from the rates of Ca^{2+} and H^+ fluxes and suggest that the antiport could be electroneutral (9). However, it cannot be excluded that ionic transports secondarily associated with the activity of the Ca^{2+}/H^+ antiport and responsible for an overall neutral charge balance, could have contributed to the measurements made.

The most striking result obtained concerned the affinity of the Ca^{2+}/H^+ antiport for Ca^{2+}. Rates of Ca^{2+} uptake were determined as a function of extravacuolar Ca^{2+} concentration from curves such as the one displayed in Figure 9. The results obtained (Fig. 10) revealed that the affinity of the antiport for Ca^{2+} (about 1.3 mM for half-saturation) was low compared to the affinities reported by Blumwald and Poole (9) for beet and by Schumaker and Sze (27) for oat tonoplast vesicles (41.7 and 10 μM, respectively). The dependency of the proton flux on external Ca^{2+} was not studied in detail. However, as expected from the operation of a proton-coupled Ca^{2+} transport, the kinetics of Ca^{2+}-induced vacuolar alkalinization with respect to Ca^{2+} concentration displayed a low affinity for Ca^{2+} rather similar to the one of Ca^{2+} uptake (results not shown).

In order to determine the possible origin of the differences between vacuoles and vesicles, a model was developed to account for the Ca^{2+} uptake by a vacuole suspension, the time course of the vacuolar alkalinization and the Ca^{2+}-dependence of Ca^{2+} uptake. This model was based on a series of assumptions described in the legend of Figure 10 namely (a) the rate of Ca^{2+} influx was driven by the *trans*-tonoplast ΔpH, (b) the rate of dissipation of the proton gradient was a function of Ca^{2+} uptake and buffering capacity of the vacuolar sap, (c) one part of the intravacuolar Ca^{2+} was complexed by citrate, and (d) the maximal Ca^{2+} accumulation was reached when ΔpH decreased and intravacuolar Ca^{2+} concentration increased to such an extent that a balance was reached between the inward and outward Ca^{2+} fluxes catalyzed by the antiport.

This model fits the experimental behavior of intact vacuoles in terms of the concentration dependence of Ca^{2+} uptake (Fig. 10, solid line), the kinetics of disappearance of Ca^{2+} from the suspension medium (Fig. 9, solid line) and the time course of vacuolar alkalinization (results not shown).

When this model was used to predict the behavior of

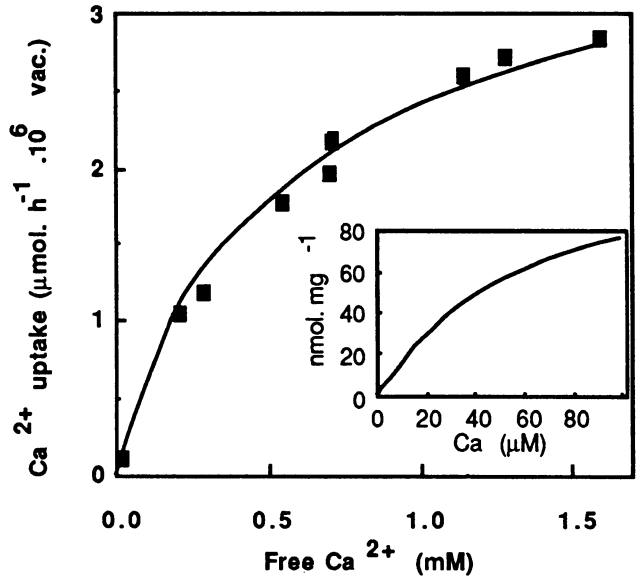

Figure 10. Concentration dependence of Ca^{2+} uptake by isolated vacuoles. Vacuoles (about 2×10^6 vacuoles·mL^{-1}) were incubated with different initial Ca^{2+} concentrations and the rates of Ca^{2+} uptake were determined from the amount of Ca^{2+} disappearing from the incubation medium during the first 2 to 5 min of uptake. Solid line represents the concentration dependence of Ca^{2+} uptake predicted by a model assuming that the Ca^{2+}/H^+ antiport was able to catalyze Ca^{2+} influx and efflux according to the relations:

$$V_{in} = (V_m \times Ca^{2+}_{out}/K_m + Ca^{2+}_{out})\,(H^+_v - H^+_{out}/H^+_{out}) \text{ and } V_{out} = V_m \times Ca^{2+}_{in}/(K_m + Ca^{2+}_{in})$$

with K_m = 1.3 mM; $V_m = 1.5 \times 10^{-6}$ nmol·min^{-1}·μm^{-2}; mean diameter = 25 μm; external pH = 7.3; vacuolar pH = 5.5; buffering power of the vacuolar sap β = 40 μEq·mL^{-1} pH unit^{-1} but increased to 60 μEq·mL^{-1} pH unit^{-1}for pHv > 6.0; intravacuolar citrate = 20 mM; mean affinity of citrate for Ca^{2+} = 0.1 mM. The rates of uptake, expressed as μmol·h^{-1}·10^6 vacuoles were calculated from the first 5 min of the simulated uptake. The same model, with the same kinetic parameters, was used to calculate what should be the concentration dependence of Ca^{2+} uptake by tonoplast vesicles, with a mean diameter of 0.33 μm, an initial *trans*-tonoplast ΔpH of 1.9 pH units (pH_{in} = 5.4) and a low buffering capacity of 4 μEq·mL^{-1} pH unit^{-1}around pH 5.5. The results are expressed as nmol of Ca^{2+} absorbed during 15 s per mg tonoplast proteins with 2×10^{-3} pg proteins·μm^{-2} (inset).

tonoplast vesicles having the same membrane properties and driving force as the vacuoles and differing only by their size (diameter: 0.33 μm), by their buffering capacity and their Ca^{2+}-complexing content, interesting results were obtained. First, the time course of Ca^{2+} uptake was strongly modified with a maximal intravesicular Ca^{2+} accumulation reached in about 10 s (Fig. 9, inset), as measured by Blumwald and Poole on beet root tonoplast vesicles (9). Second, the concentration dependence of Ca^{2+} uptake was also modified in vesicles (Fig. 10, inset) compared to vacuoles with a drastic shift of the apparent K_m toward much lower values (50–70 μM instead of 1.3 mM for vacuoles) in rather good agreement with the experimental results published by Blumwald and Poole (9). Furthermore, the model predicted that 0.3 μm vesicles with an initial ΔpH of 1.9 pH unit should display a maximum rate of accumulation of 40 nmol Ca^{2+}·mg^{-1} protein·min^{-1} with an apparent K_m of 40 μM, not so far from the results obtained by Schumaker and Sze with oat root tonoplast vesicles (27).

Thus, the model gave a reasonably good representation of the experimentally observed differences in the behavior of vesicles compared to intact vacuoles. It appeared that the high surface to volume ratio of vesicles allows a fast buildup of a Ca^{2+} concentration gradient and a fast dissipation of the transmembrane ΔpH which also depends on the low intravesicular buffering capacity in the pH range 5.5 to 6.5. The maximum accumulation capacity of the vesicles can be reached within less than 1 min, even for low external Ca^{2+} concentrations, the limiting factor in the accumulation of Ca^{2+} being the drop in ΔpH and not the saturation of the antiport. The consequences are (a) the difficulty to measure real initial rates of uptake, (b) the strong shift in the apparent affinity of the antiport for Ca^{2+}, and (c) the increase of the apparent initial rates of Ca^{2+} uptake in vacuoles compared to vesicles (2.4; 16.8 and 60–120 μmol·h^{-1}·mg^{-1} protein for oat root vesicles (27), beet root vesicles (9) and *C. roseus* vacuoles respectively, for 100 μM external Ca^{2+}).

The next puzzling question to consider is the biological significance of a Ca^{2+}-antiport with a low affinity (about 1 mM) facing cytoplasmic Ca^{2+} concentrations at least three orders of magnitude lower. The Ca^{2+} uptake catalyzed by the Ca^{2+}/H^+ antiport located at the tonoplast of one vacuole, 25 μm in diameter, removing Ca^{2+} from a cytoplasmic compartment with a calcium concentration of 1 μM and a relative volume of 10% of the vacuolar one was calculated under different conditions. The results obtained using the kinetic parameters reported for oat root vesicles (V_{max} = 40 nmol·min^{-1}·mg^{-1}; K_m = 10 μM), for beet root vesicles (V_{max} = 400 nmol·min^{-1}·mg^{-1}; K_m = 40 μM) and those obtained here for *C. roseus* vacuoles (V_{max} = 18 μmol·min^{-1}·mg^{-1}; K_m = 1.3 mM) were, respectively, 1.8×10^{-5}, 4.8×10^{-5}, and 6.9×10^{-5} pmol·min^{-1}·vacuole^{-1}. When compared to the estimate of the cytoplasmic Ca^{2+} content (about 8×10^{-7} pmol for a volume of 800 μm^3 and a concentration of 1 μM), these rates show that the antiport, whichever set of kinetic parameters choosen, is potentially able to remove most of the cytoplasmic calcium within less than 5 s. Calculations made for a cytoplasmic Ca^{2+} concentration of 0.1 μM gave about the same results. The apparently paradoxical agreement between the results of the calculations made starting from the vesicular situation or from the vacuolar situation comes from the balanced consequences of the fast ΔpH dissipation in vesicles which lowers the accumulation (*i.e.* the apparent V_{max}) but at the same time increases markedly the apparent affinity.

Thus, the interesting conclusion of this study is that, despite its low affinity for calcium, the Ca^{2+}/H^{2+} antiport of *C. roseus* vacuole has such a high capacity for Ca^{2+} uptake that it has a strong potential ability to regulate the concentration of calcium in the cytoplasm.

CONCLUSIONS

Beet tonoplast vesicles have been extensively studied with respect to the systems involved in the exchange of protons and proton-equivalents across the tonoplast and four of these systems, namely the H^+-ATPase, the H^+-PPase, the Na^+/H^+, and the Ca^{2+}/H^+ antiports have all been characterized using this material (3, 4, 8, 9, 25). *C. roseus* is the second plant

species for which these four major transport systems for protons and cations have been shown to be present on the vacuolar membrane.

One of the original features of this study was to use isolated vacuoles with a low surface to volume ratio. This property was responsible for the rather slow changes observed in the intravacuolar H^+, Ca^{2+}, or Na^+ concentrations. However, due to the important activity of the H^+-exchange systems per unit surface of the tonoplast membrane and because of the large vacuolar volume compared to the cytoplasmic one, the amount of ions exchanged were high and potentially corresponded to dramatic modifications of the concentrations of H^+, Na^+, and Ca^{2+} in the cytoplasm. This could explain how the Ca^{2+}/H^+ antiport, operating far from the Ca^{2+} -saturating concentration, can efficiently contribute to the regulation of free Ca^{2+} in the cytoplasm.

As to the buffering power of the vacuolar sap, the results obtained show that its capacity to resist pH modifications linked to the exchange of protons or proton-equivalents across the tonoplast is low compared to the activity of the H^+-transport systems. Thus, the regulation of vacuolar pH appears as a dynamic process with only a limited contribution of the buffering properties of the intravacuolar sap. However, the interaction between the buffering power of the vacuolar sap and the regulation of vacuolar pH is certainly more complex as the exchange of malate (one of the buffering component of the vacuolar sap) across the tonoplast has been shown to be important in regulating the intravacuolar pH and determining its variability in cell populations (15 and reference therein). Furthermore, as discussed above for the uptake and accumulation of Ca^{2+} by isolated vacuoles, the buffering power of the vacuolar sap, in cooperation with the presence of Ca^{2+}-complexing anions, can be a factor in the amplification of ion accumulation when the uptake of these ions is both dissipating the *trans*-tonoplast ΔpH and ΔpH-driven.

A rather complex picture of the regulation of vacuolar pH emerges from studies in recent years as several antagonistic systems exchanging protons and proton-equivalents between the cytoplasm and the vacuolar compartment have been described. Only some of them have been studied here and further experiments are needed to identify the entire set of components of this system. Furthermore, the different translocators involved in the vacuolar pH regulation have been, up to now, considered independently of each other and the interactions between the components of this regulating system should now be studied.

LITERATURE CITED

1. **Admon A, Jacoby B, Goldschmitt EE** (1981) Some characteristics of the Mg-ATPase of isolated beet vacuoles. Plant Sci Lett **22:** 89–96
2. **Auderset G, Sandelius AS, Penel C, Brightman A, Greppin H, Morre J** (1986) Isolation of plasma membrane and tonoplast fractions from spinach leaves by preparative free-flow electrophoresis and effect of photoinduction. Physiol Plant **68:** 1–12
3. **Bennett AB, O'Neill SD, Spanswick RM** (1984) H^+-ATPase activity from storage tissue of Beta vulgaris. I- Identification and characterization of an anion-sensitive H^+-ATPase. Plant Physiol **74:** 538–544
4. **Bennett AB, Spanswick RM** (1984) H^+-ATPase activity from storage tissue of *Beta vulgaris*. II-H^+/ATP stoichiometry of an anion-sensitive H^+-ATPase. Plant Physiol **74:** 545–548
5. **Bentrup FW, Gogarten-Boekels MM, B Hoffmann, JP Gogarten, Baumann C** (1986) ATP-dependent acidification and tonoplast hyperpolarization of isolated vacuoles from green supension cells of *Chenopodium rubrum*. Proc Natl Acad Sci USA **83:** 2431–2433
6. **Blumwald E** (1987) Tonoplast vesicles as a tool in the study of ion transport at the plant vacuole. Physiol Plant **69:** 731–734
7. **Blumwald E, Cragoe EJ, Poole RJ** (1987) Inhibition of Na^+/H^+ antiport activity in sugar beet tonoplast by analogs of amiloride. Plant Physiol **85:** 30–33
8. **Blumwald E, Poole rj** (1985) Na^+/H^+ antiport in isolated tonoplast vesicles from storage tissue of *Beta vulgaris*. Plant Physiol **78:** 163–167
9. **Blumwald E, Poole RJ** (1986) Kinetics of Ca^{2+}/H^+ antiport in isolated tonoplast vesicles from storage tissue of *Beta vulgaris* L. Plant Physiol **80:** 727–731
10. **Briskin DP, Thornley WR, Wyse RE** (1985) Membrane transport in isolated vesicles from sugar beet taproot. I- Isolation and characterization of energy dependent H^+-transporting vesicles. Plant Physiol **78:** 865–870
11. **Busch DR, SZE H** (1986) Calcium transport in tonoplast and endoplasmic reticulum vesicles isolated from cultured carrot cells. Plant Physiol **80:** 549–555
12. **Chanson A, Fichmann J, Spear D, Taiz L** (1985) Pyrophosphate-driven proton transport by microsomal membranes of corn coleoptiles. Plant Physiol **79:** 159–164
13. **Colombo R, Cerana R, Lado P** (1987) Mg-ATP-dependent H^+ transport in vacuoles and tonoplast vesicles from *Acer pseudoplatanus* cells. *In* Plant Vacuoles. Their Importance in Solute Compartmentation in Cells and Their Applications in Plant Biotechnology. B. Marin, ed, NATO ASI Series, Vol 134, Plenum Press, New York, pp 191–198
14. **Kurkdjian A, Manigault P, Manigault J, Guern J** (1984) Action of fusicoccin on the vacuolar pH of *Acer pseudoplatanus* as evidenced by 9-aminoacridine microfluorimetry. Plant Sci Lett **34:** 1–5
15. **Kurkdjian A, Quiquampoix H, Barbier-Brygoo H, Pean M, Manigault P, Guern J** (1985) Critical evaluation of methods for estimating the vacuolar pH of plant cells. *In* Biochemistry and Function of Vacuolar ATPase in Fungi and plant cells. B Marin, ed, Springer-Verlag, Berlin, pp 98–113
16. **Leigh RA, Walker RR** (1980) ATPase and acid phosphatase activities associated with vacuoles isolated from storage roots of red beet (*Beta vulgaris* L.). Planta **150:** 222–229
17. **Leigh RA, Pope AJ** (1987) Understanding tonoplast function: some emerging problems. *In* Plant Vacuoles. Their Importance in Solute Compartmentation in Cells and Their Applications in Plant Biotechnology. B Marin ed., NATO ASI Series, Vol 134, Plenum Press, New York, pp 101–110
18. **Lew RR, Spanswick RM** (1985) Characterization of anion effects on the nitrate-sensitive ATP-dependent proton pumping activity of soybean (*Glycine max* L.) seedling root microsomes. Plant Physiol **77:** 352–357
19. **Lin W, Wagner GJ, Siegelman HW, Hind G** (1977) Membrane-bound ATP of intact vacuoles and tonoplasts isolated from mature plant tissue. Biochim. Biophys Acta **465:** 110–117
20. **Manigault P, Manigault J, Kurkdjian A** (1983) A fluorimetric method for vacuolar pH measurement in plant cells using 9-aminoacridine. Physiol Vég **21:** 129–136
21. **Martin JB, Klein G, Satre M** (1987) ^{23}Na NMR study of intracellular sodium ions in *Dictyostelium discoideum* amaeba. Arch Biochem Biophys **254:** 559–567
22. **Mathieu Y, Guern J, Kurkdjian A, Manigault P, Manigault J, Zielinska T, Gillet B, Beloeil J-C, Lallemand J-Y** (1988) Regulation of vacuolar pH of plant cells. I. Isolation and properties of vacuoles suitable for ^{31}P NMR studies. Plant Physiol (in press)
23. **Niemitz C, Willenbrink J** (1985) The function of the tonoplast ATPase in intact vacuoles of red beet is governed by direct and indirect ion effects. Planta **166:** 545–549
24. **Pugin A, Montrichard F, Le-Quoc K, Le-Quoc D** (1986) Incidence of the method for the preparation of vacuoles on the

vacuolar ATPase activity of isolated *Acer pseudoplatanus* cells. Plant Sci **47:** 165–172
25. **Rea PA, Poole RJ** (1985) Proton-translocating inorganic pyrophosphatase in red beet (*Beta vulgaris* L.) tonoplast vesicles. Plant Physiol **77:** 46–52
26. **Rea PA, Sanders D** (1987) Tonoplast energization: Two H^+ pumps, one membrane. Physiol Plant **71:** 131–141
27. **Schumaker KS, Sze H** (1986) Calcium transport into the vacuole of oat roots. Characterization of H^+/Ca^{2+} exchange activity. J Biol Chem **161:** 12172–12178
28. **Sze H** (1985) H^+-translocating ATPases: advances using membranes vesicles. Annu Rev Plant Physiol **36:** 175–208
29. **Thom M, Komor E** (1985) Electrogenic proton translocation by the ATPase of sugarcane vacuoles. Plant Physiol **77:** 329–334
30. **Tu S-I, Naghashi G, Brouillette JN** (1987) Proton pumping kinetics and origin of nitrate inhibition of tonoplast-type H^+ ATPase. Arch Biochem Biophys **126:** 625–637
31. **Wagner GJ, Mulready P** (1983) Characterization and solubilisation of nucleotide specific Mg^{2+}-ATPase and Mg^{2+}-pyrophosphatase of tonoplast. Biochim Biophys Acta **728:** 267–280
32. **Walker RR, Leigh RA** (1981) Characterization of a salt-stimulated ATPase activity associated with vacuoles isolated from storage roots of red beet (*Beta vulgaris* L.) Planta **153:** 140–149
33. **Wang Y, Leigh RA, Kaestner KH, Sze H** (1986) Electrogenic H^+ pumping pyrophosphatase in tonoplast vesicles of oat roots. Plant Physiol **81:** 497–502